

PNNL-31038

# Thermocatalytic Heat Pipes for Geothermal Resource Recovery

October 2020

B. Peter McGrail (PI)  
Mark D. White  
Signe White  
Jian Liu  
Satish K. Nune  
Jeromy J. Jenks

## DISCLAIMER

This report was prepared as an account of work sponsored by an agency of the United States Government. Neither the United States Government nor any agency thereof, nor Battelle Memorial Institute, nor any of their employees, makes **any warranty, express or implied, or assumes any legal liability or responsibility for the accuracy, completeness, or usefulness of any information, apparatus, product, or process disclosed, or represents that its use would not infringe privately owned rights.** Reference herein to any specific commercial product, process, or service by trade name, trademark, manufacturer, or otherwise does not necessarily constitute or imply its endorsement, recommendation, or favoring by the United States Government or any agency thereof, or Battelle Memorial Institute. The views and opinions of authors expressed herein do not necessarily state or reflect those of the United States Government or any agency thereof.

PACIFIC NORTHWEST NATIONAL LABORATORY  
*operated by*  
BATTELLE  
*for the*  
UNITED STATES DEPARTMENT OF ENERGY  
*under Contract DE-AC05-76RL01830*

Printed in the United States of America

Available to DOE and DOE contractors from the  
Office of Scientific and Technical Information,  
P.O. Box 62, Oak Ridge, TN 37831-0062;  
ph: (865) 576-8401  
fax: (865) 576-5728  
email: [reports@adonis.osti.gov](mailto:reports@adonis.osti.gov)

Available to the public from the National Technical Information Service  
5301 Shawnee Rd., Alexandria, VA 22312  
ph: (800) 553-NTIS (6847)  
email: [orders@ntis.gov](mailto:orders@ntis.gov) <<https://www.ntis.gov/about>>  
Online ordering: <http://www.ntis.gov>

# **Thermocatalytic Heat Pipes for Geothermal Resource Recovery**

October 2020

B. Peter McGrail (PI)  
Mark D. White  
Signe White  
Jian Liu  
Satish K. Nune  
Jeromy J. Jenks

Prepared for  
the U.S. Department of Energy  
under Contract DE-AC05-76RL01830

Pacific Northwest National Laboratory  
Richland, Washington 99354

## Abstract

Heat pipes are an important technology that allow orders of magnitude faster heat transfer than simple conduction. However, operating principles in heat pipes place fundamental bounds on their performance (critical heat flux and efficiency). Conventional heat pipe functionality is inherently tied to vaporization and condensation of the working fluid charged in the heat pipe. These fluids each have different operating temperature ranges based on the capillary, entrainment, sonic, and boiling limits of the heat pipe design. These limits, typically the capillary limit, dictate the maximum heat flux a heat pipe can carry, and most importantly for geothermal systems, the distance over which the pipes can operate (100 to 200 m maximum under optimum conditions). A thermocatalytic heat pipe breaks the inherent limitations of phase change thermo- and hydrodynamics and can transform heat pipe technology as a potentially more efficient means of extracting heat from a geothermal resource.

The thermocatalytic heat pipe uses a working fluid to transport both sensible and chemical heat. An endothermic chemical reaction at depth removes heat from the reservoir and produces reactive intermediates, which are transported to the surface and used to run a reverse exothermic reaction that releases heat for use in power generation or other useful purposes. This technology offers two distinct advantages over conventional geothermal heat recovery technologies: (1) lower heat loss to the rock outside of the geothermal reservoir, and (2) higher heat transfer rates to the well field within the geothermal reservoir. Both advantages offer opportunity to reduce risks and lower costs of geothermal energy recovery.

In this report, we discuss an initial effort to assess the efficacy and limitations of this technology for extracting heat from both porous/permeable and nominally impermeable geothermal reservoirs. Numerical simulation capabilities of the STOMP-GT code were enhanced to enable simulations of thermochemical heat pipes traversing geothermal reservoirs. An array of potential thermochemical reaction systems was evaluated and screened. Of these, an ethanol dehydration reaction was most promising in the vapor-liquid reaction set. A solid-phase dehydration reaction ( $\text{CuSO}_4 \cdot 5\text{H}_2\text{O}$ ) showed the highest reaction enthalpy per unit volume but would require development of a nonaqueous carrier fluid to implement it in a heat pipe. Subsurface reservoir simulations predicted long-term performance of the heat pipes for each geothermal reservoir type. The performance of U-shaped wells and coaxial wells was evaluated for a suite of reactions for both hydrothermal and hot dry rock reservoirs and was compared with a baseline case of simply pumping water through the wells. The heat pipe technology was additionally evaluated for an enhanced geothermal system (EGS) with an injection borehole, production borehole, and intervening hydraulically conductive fracture. All reservoir types showed significant improvement in heat recovered over a 20-year operating period ranging from a 1.8X increase for the hot dry rock case to more than 2.5X more energy recovered for the EGS case.



Contents

Abstract.....iii

Thermocatalytic Heat Pipes for Geothermal Resource Recovery..... 1

Reservoir Simulation ..... 2

Reversible Thermochemical Reactions and Reaction System Assessment..... 11

Summary..... 15

Overall Conclusions and Recommendations ..... 15



## Thermocatalytic Heat Pipes for Geothermal Resource Recovery

October 29, 2020

B. Peter McGrail (PI)

Mark D. White

Signe White

Jian Liu

Satish K. Nune

Jeremy J. Jenks



PNNL is operated by Battelle for the U.S. Department of Energy



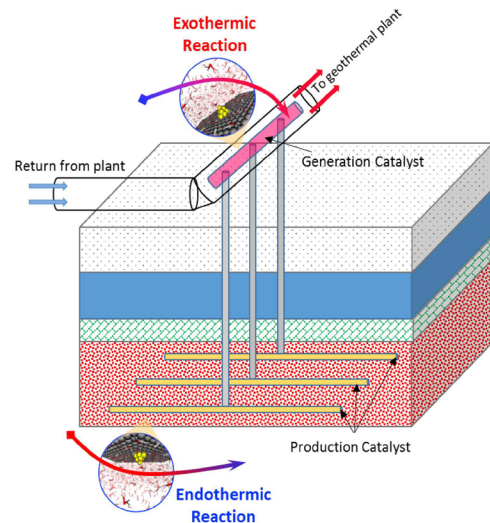
## Project Overview

### Scope

- Conduct simulations of a new class of heat pipe that enables nearly lossless transport of heat from deep geothermal reservoirs
- Instead of vapor-liquid condensation, thermochemical reactions with 10 to 50X higher heat carrying capacity are used to extract heat from the hot end of the heat pipe and produce reactive intermediates, which are transported to the "cold" end for heat recovery at the surface with a reverse reaction
- Heterogeneous catalysts (if required) are used in the heat pipe to control position where the thermochemical reactions occur

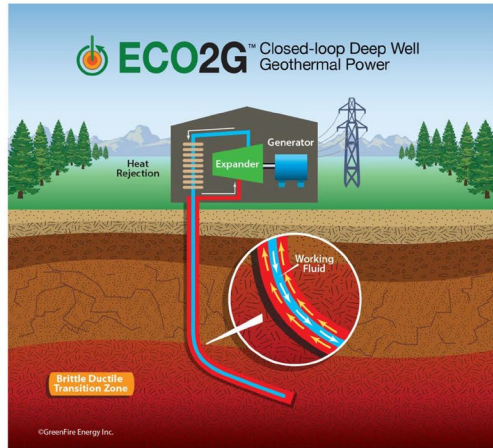
### Project Impacts

- Geothermal resource recovery virtually anywhere
- Enable chemical heat pumping to thermally upgrade heat sources
- Reduce geothermal development risk due to adverse subsurface reservoir properties
- Reduce regulatory barriers and public perception concerns over fracking for EGS
- Eliminate surface heat exchanger fouling and maintenance issues from silica (and other mineral) precipitation
- Potentially reduce wellfield development costs with slim hole drilling techniques for heat pipes

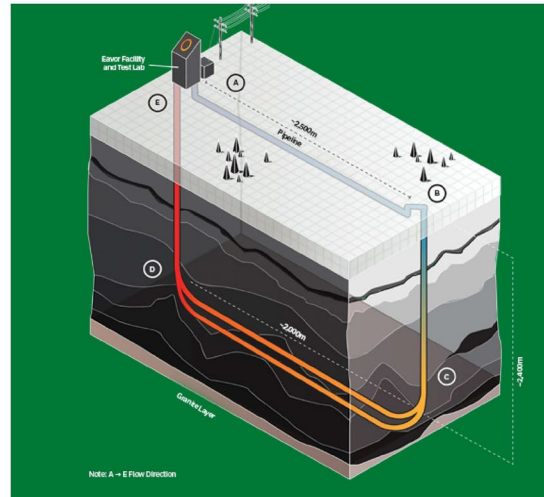




## Greenfire Energy



## Eavor



3

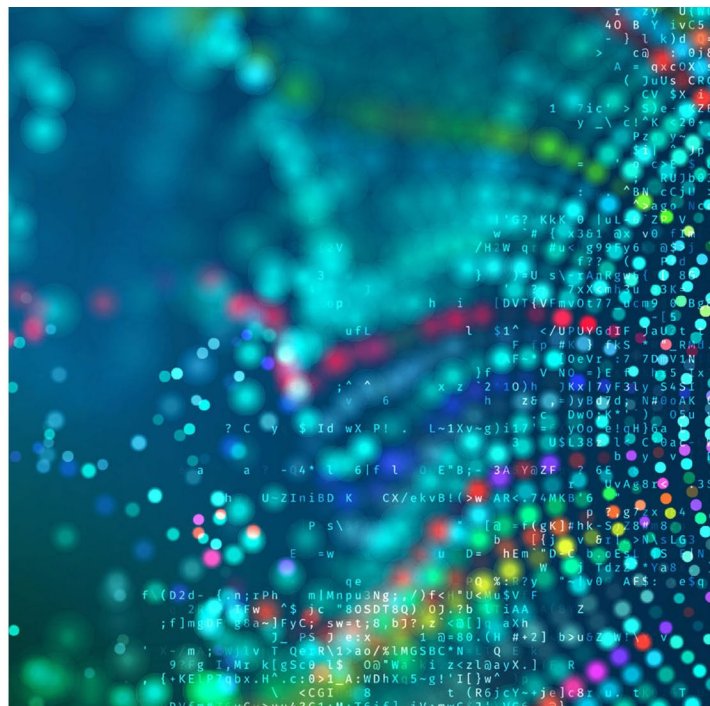


## Reservoir Simulation

**Mark White**  
**Signe White**

Geophysics and Geomechanics  
Pacific Northwest National Laboratory

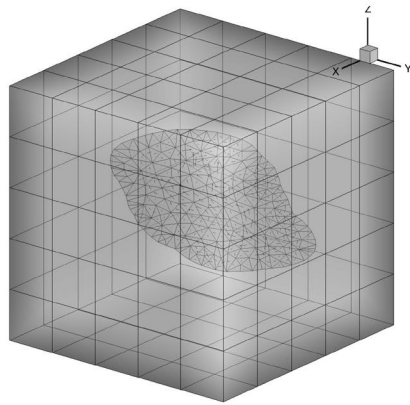
U.S. DEPARTMENT OF  
**ENERGY** **BATTELLE**  
PNNL is operated by Battelle for the U.S. Department of Energy



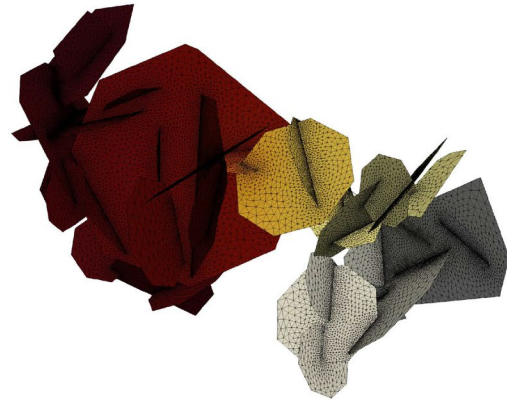
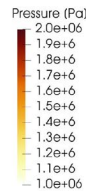




## Embedded Borehole and Fracture Modeling w/ STOMP-GT



Discretized fracture embedded within a discretized rock matrix

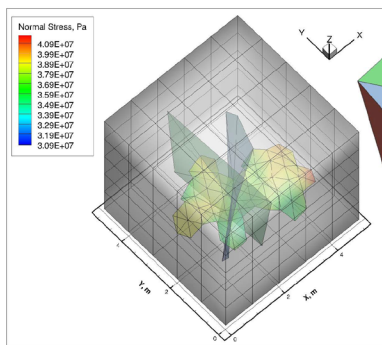


dfnWorks (LANL) discrete fracture network model with a conforming grid without a surrounding rock matrix

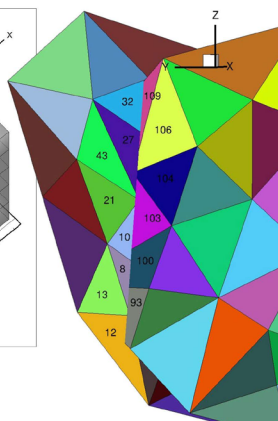
5



## Embedded Borehole and Fracture Modeling w/ STOMP-GT



Discretized fractures embedded within a discretized rock matrix

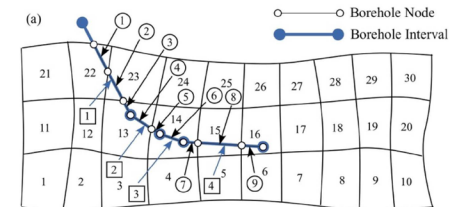
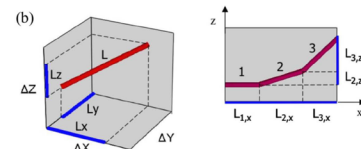


Fracture-fracture connection mapping

$$W_{Lx} = \left[ \frac{2\pi\sqrt{k_y k_z} L_z}{\ln\left(\frac{2\pi\sqrt{k_y k_z} L_z}{\ln\left(\frac{2\pi\sqrt{k_y k_z} L_z}{r_{0,x}}\right)}\right)} \right]; W_{Ly} = \left[ \frac{2\pi\sqrt{k_x k_z} L_z}{\ln\left(\frac{2\pi\sqrt{k_x k_z} L_z}{\ln\left(\frac{2\pi\sqrt{k_x k_z} L_z}{r_{0,y}}\right)}\right)} \right]; W_{Lz} = \left[ \frac{2\pi\sqrt{k_x k_y} L_z}{\ln\left(\frac{2\pi\sqrt{k_x k_y} L_z}{\ln\left(\frac{2\pi\sqrt{k_x k_y} L_z}{r_{0,z}}\right)}\right)} \right]$$

$$r_{0,x} = \left[ \frac{\left(\frac{k_y}{k_x}\right)^{1/2} \Delta x^2 + \left(\frac{k_z}{k_x}\right)^{1/2} \Delta y^2}{\left(\frac{k_y}{k_x}\right)^{1/2} + \left(\frac{k_z}{k_x}\right)^{1/2}} \right]^{1/2}; r_{0,y} = \left[ \frac{\left(\frac{k_x}{k_y}\right)^{1/2} \Delta x^2 + \left(\frac{k_z}{k_y}\right)^{1/2} \Delta y^2}{\left(\frac{k_x}{k_y}\right)^{1/2} + \left(\frac{k_z}{k_y}\right)^{1/2}} \right]^{1/2}; r_{0,z} = \left[ \frac{\left(\frac{k_x}{k_z}\right)^{1/2} \Delta x^2 + \left(\frac{k_y}{k_z}\right)^{1/2} \Delta y^2}{\left(\frac{k_x}{k_z}\right)^{1/2} + \left(\frac{k_y}{k_z}\right)^{1/2}} \right]^{1/2}$$

$$W_I = \sqrt{(W_{Lx})^2 + (W_{Ly})^2 + (W_{Lz})^2}$$

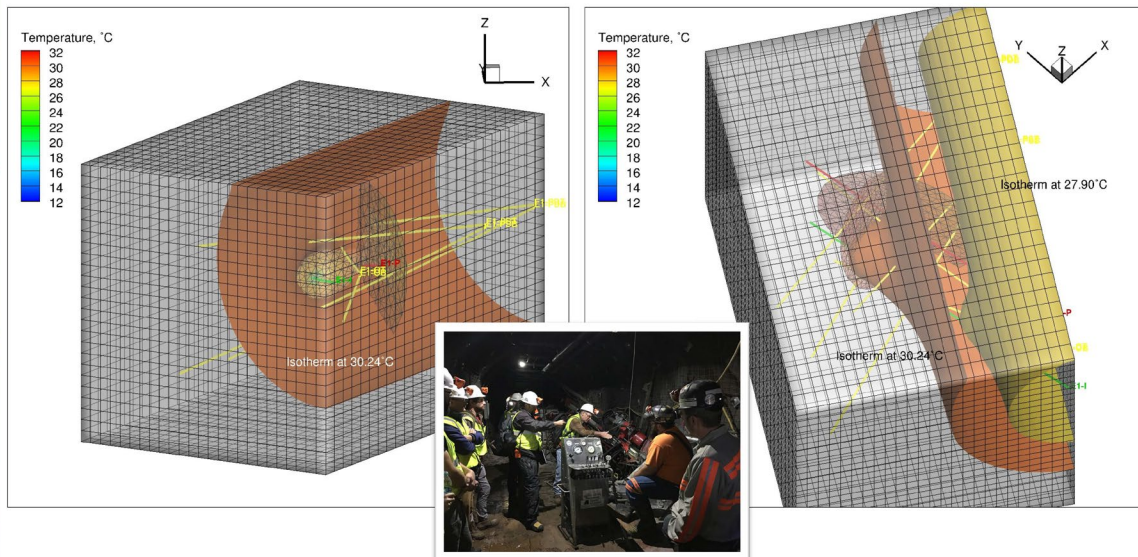


Borehole trajectories translated into borehole nodes

6



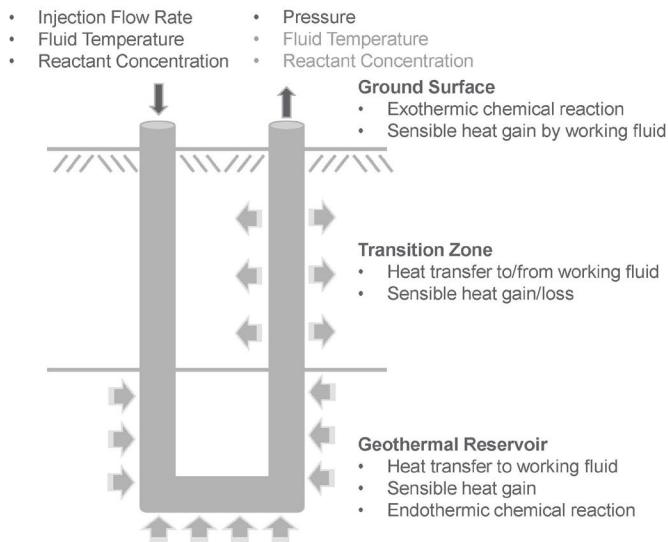
## Embedded Borehole and Fracture Modeling w/ STOMP-GT



7



## U-Pipe Modeling Approaches and Concepts



### Pipe Flow

- Darcy-Weisbach Equation
- Colebrook Equation

$$\Delta P = \lambda \frac{L}{D_h} \frac{\rho u^2}{2}$$

$$\frac{1}{\sqrt{\lambda}} = -2 \log \left[ \frac{2.51}{Re \sqrt{\lambda}} + \frac{r_f}{3.72 D_h} \right]$$

### Heat Transfer

- Peaceman conduction model between outer pipe wall and rock matrix
- Radial conduction across pipe wall
- Fully developed flow advection between inner pipe wall and working fluid

### Endothermic Chemical Reaction

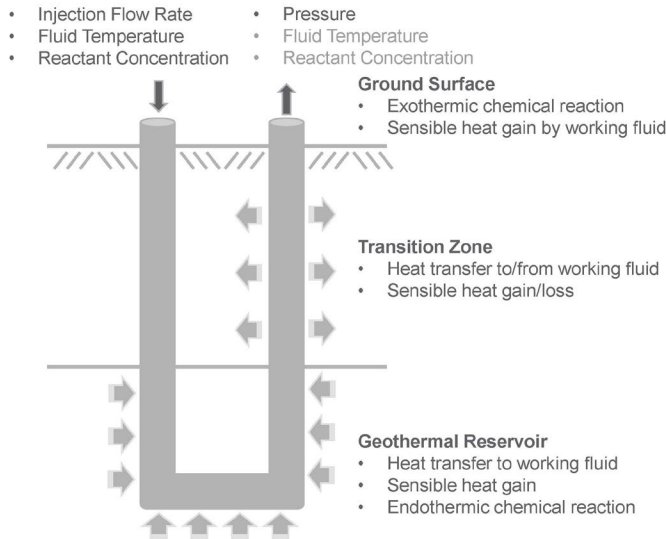
- Temperature controlled first-order reaction rate

$$r = \frac{k [C_s]}{\left( 1 + \exp \left( \frac{(T^* - T)}{\beta} \right) \right)}$$

8



## U-Pipe Modeling Approaches and Concepts



### Pipe Flow

- Darcy-Weisbach Equation
- Colebrook Equation

$$\Delta P = \lambda \frac{L}{D_h} \frac{\rho u^2}{2}$$

$$\frac{1}{\sqrt{\lambda}} = -2 \log \left[ \frac{2.51}{Re \sqrt{\lambda}} + \frac{r_f}{3.72 D_h} \right]$$

### Heat Transfer

- Peaceman conduction model between outer pipe wall and rock matrix
- Radial conduction across pipe wall
- Fully developed flow advection between inner pipe wall and working fluid

### Endothermic Chemical Reaction

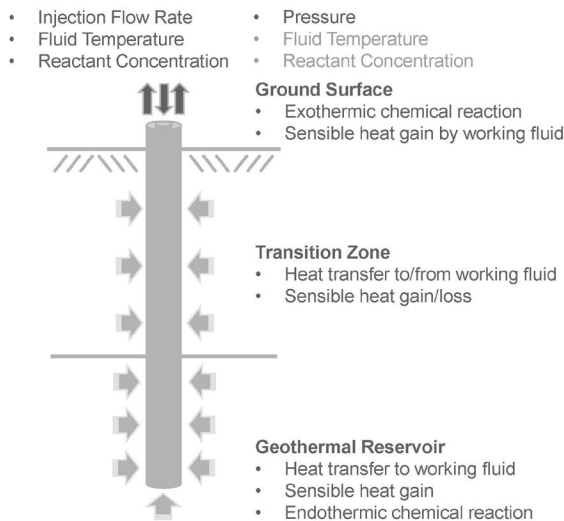
- Temperature controlled first-order reaction rate

$$r = \frac{k [C_s]}{\left( 1 + \exp \left( \frac{(T^* - T)}{\beta} \right) \right)}$$

8



## Coaxial-Pipe Modeling Approaches and Concepts



### Pipe Flow

- Darcy-Weisbach Equation
- Colebrook Equation

$$\Delta P = \lambda \frac{L}{D_h} \frac{\rho u^2}{2}$$

$$\frac{1}{\sqrt{\lambda}} = -2 \log \left[ \frac{2.51}{Re \sqrt{\lambda}} + \frac{r_f}{3.72 D_h} \right]$$

### Heat Transfer

- Peaceman conduction model between outer-outer pipe wall and rock matrix
- Radial conduction across outer pipe wall
- Fully developed flow advection between inner-outer pipe wall and working fluid
- Fully developed flow advection between outer-inner pipe wall and working fluid
- Radial conduction across inner pipe wall
- Fully developed flow advection between inner-inner pipe wall and working fluid

### Endothermic Chemical Reaction

- Temperature controlled first-order reaction rate

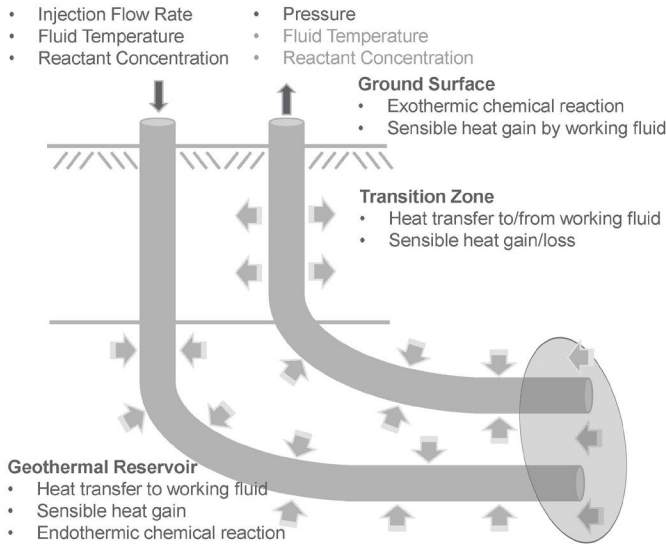
$$r = \frac{k [C_s]}{\left( 1 + \exp \left( \frac{(T^* - T)}{\beta} \right) \right)}$$

9





## EGS Modeling Approaches and Concepts



### Pipe Flow

- Darcy-Weisbach Equation
- Colebrook Equation

$$\Delta P = \lambda \frac{L}{D_h} \frac{\rho u^2}{2}$$

$$\frac{1}{\sqrt{\lambda}} = -2 \log \left[ \frac{2.51}{Re \sqrt{\lambda}} + \frac{r_f}{3.72 D_h} \right]$$

### Heat Transfer

- Peaceman conduction model between outer pipe wall and rock matrix
- Peaceman conduction model between fracture plane and rock matrix
- Radial conduction across pipe wall
- Fully developed flow advection between inner pipe wall and working fluid

### Endothermic Chemical Reaction

- Temperature controlled first-order reaction rate

$$r = \frac{k [C_s]}{\left( 1 + \exp \left( \frac{(T^* - T)}{\beta} \right) \right)}$$

10



## Computing and Comparing Outputs

### Water vis-à-vis Thermocatalytic Fluid

- Water

$$P = \dot{m} (h_o - h_i)$$

$$P_{Carnot} = P \left( 1 - \frac{T_i}{T_o} \right)$$

$$E_{Carnot} = \int P_{Carnot} dt$$

- Thermocatalytic Fluid

$$P = \dot{m} (h_o - h_i + \Delta h_{reaction})$$

$$T'_o = T_{sat} (h_o + \varepsilon \Delta h_{reaction})$$

$$P_{Carnot} = P \left( 1 - \frac{T_i}{T'_o} \right)$$

$$E_{Carnot} = \int P_{Carnot} dt$$

Value of the Power Produced

Value of the Power Produced

$E_{Carnot}$  - integrated Carnot efficiency x power, J

$h_i$  - enthalpy of inlet water, J/kg

$h_o$  - enthalpy of outlet water, J/kg

$\Delta h_{reaction}$  - heat of reaction, J/kg

$\dot{m}$  - mass flow rate, kg/s

$P$  - produced power, W

$P_{Carnot}$  - Carnot efficiency x produced power, W

$t$  - time, s

$T_i$  - inlet temperature, K

$T_o$  - outlet temperature, K

$T_{sat}$  - saturated liquid water temperature at enthalpy, K

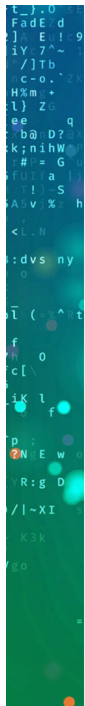
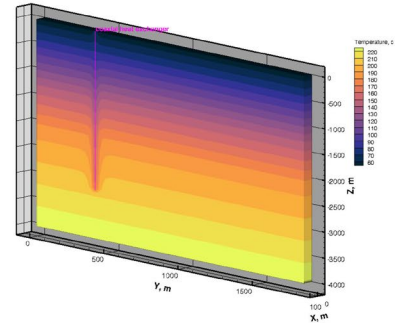
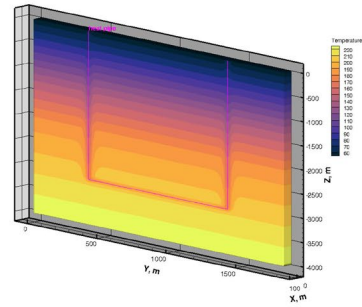
$\varepsilon$  - reaction conversion efficiency (assumed 1.0)

11

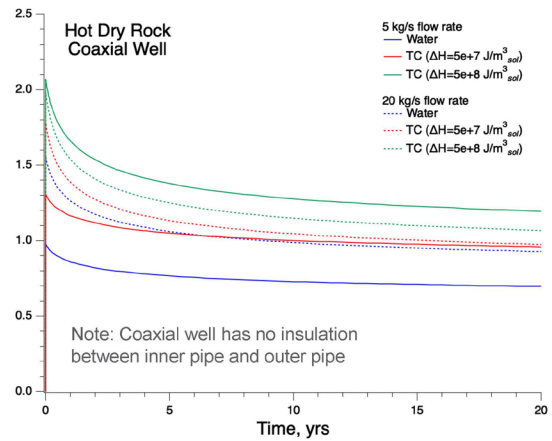
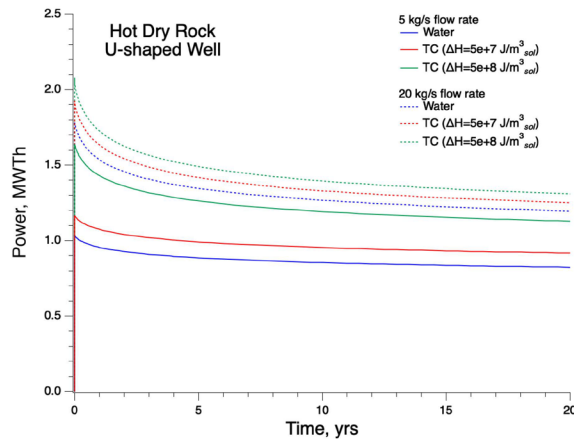


## Hot Dry Rock

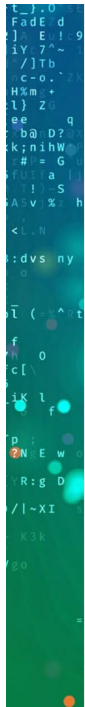
- Model based on data from FORGE deep well site
- U-shaped well and coaxial well (with no insulation between inner and outer pipes)
- Depth to horizontal section of well = 3015 m
- Temperature at bottom of reservoir = 230° C
- Flow rates 5 kg/s and 20 kg/s



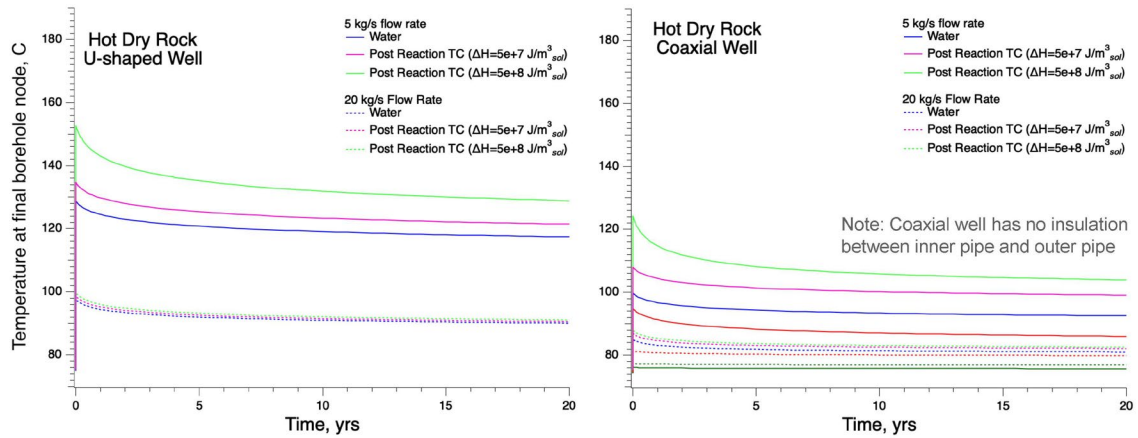
## Hot Dry Rock Simulation Results



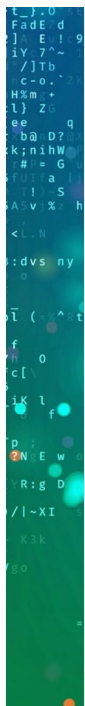




## Hot Dry Rock Simulation Results

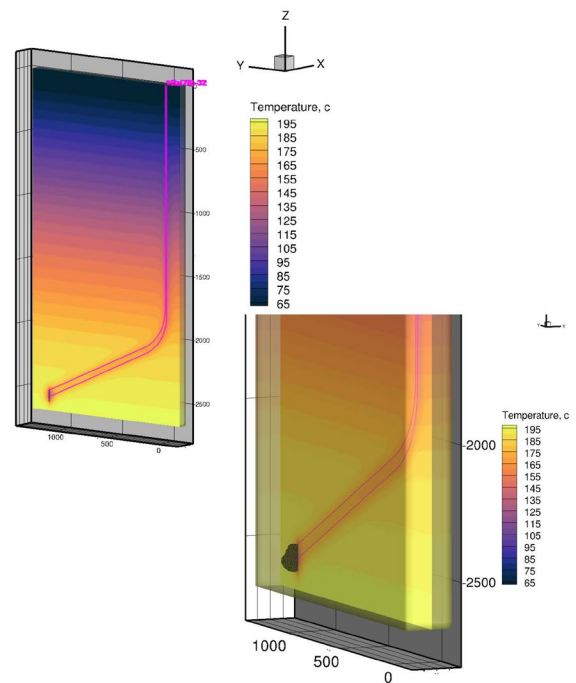


14



## EGS Utah Forge

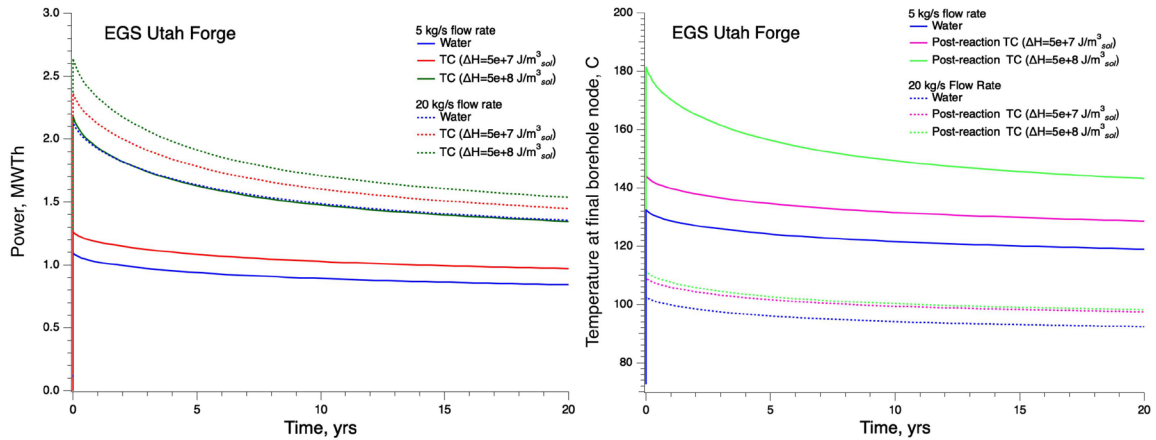
- Model based on Utah FORGE EGS with two boreholes 16A(78)-32 and 16B(78)-32, connected by a fracture with a 50-m radius
- Depth to bottom of wells = 2585 m
- Temperature at bottom of reservoir = 230°C
- Flow rates 5 kg/s and 20 kg/s



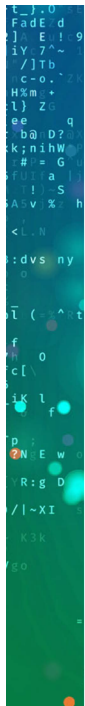
15



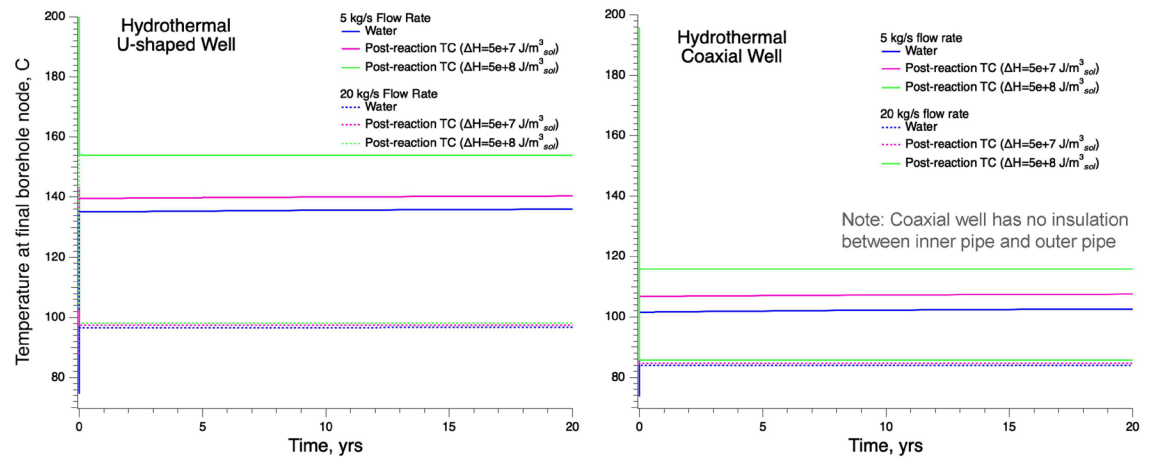
## EGS Utah Forge Simulation Results



16



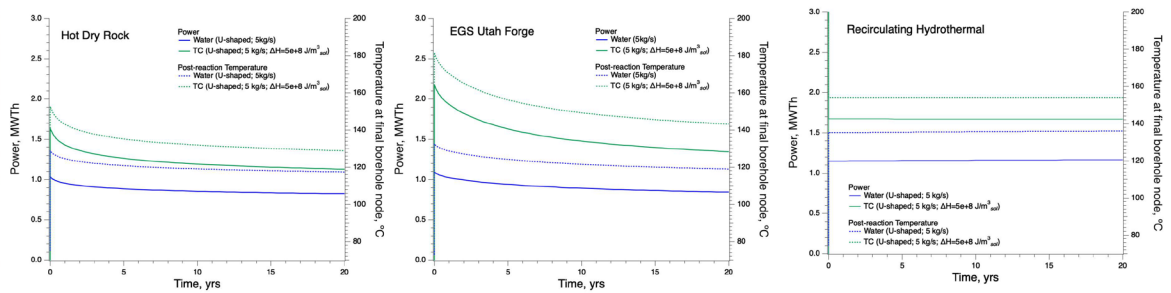
## Recirculating Hydrothermal Simulation Results



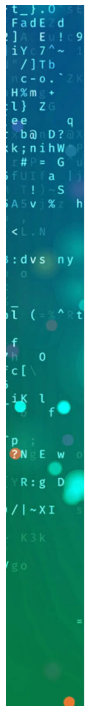
19



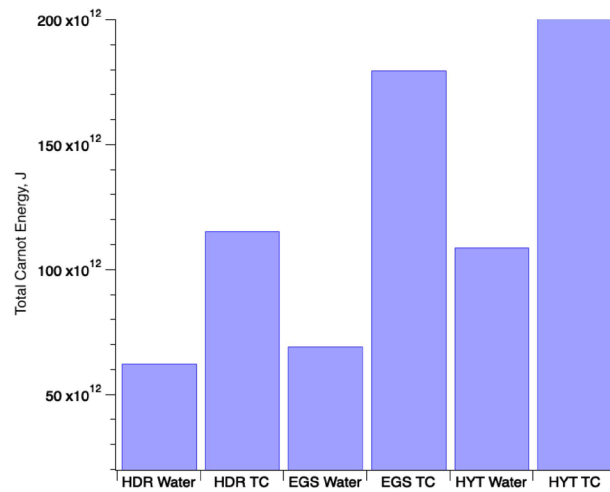
## Summary of Best Cases based on Carnot Power



20



## Summary of Total Carnot Energy produced over 20 years



21

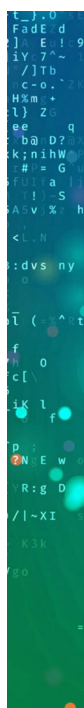
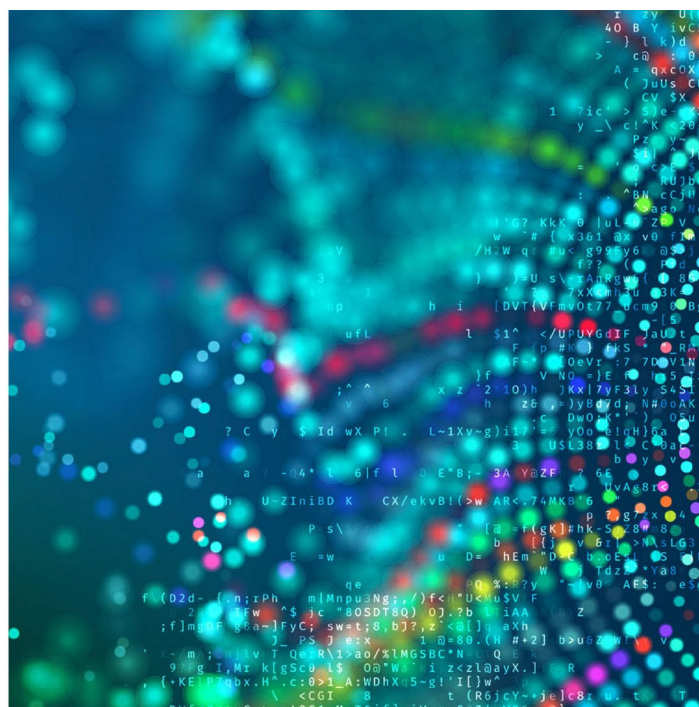


# Reversible Thermochemical Reactions and Reaction System Assessment

Jian Liu  
Satish Nune

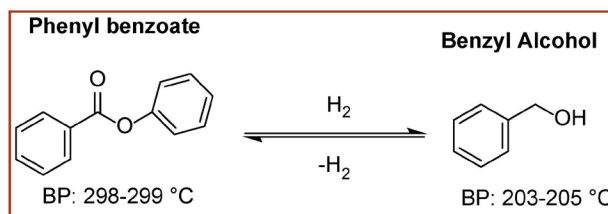
U.S. DEPARTMENT OF  
ENERGY **BATTELLE**

PNNL is operated by Battelle for the U.S. Department of Energy



## Reversible Thermochemical Reactions: Heat Pipes

- ❖ High heat of reaction (Exothermic)
- ❖ Boiling point temperature difference between the two components should be large enough so phase difference exists.
- ❖ Faster kinetics (reversibility)
- ❖ Minimal degradation
- ❖ High operation temperature.

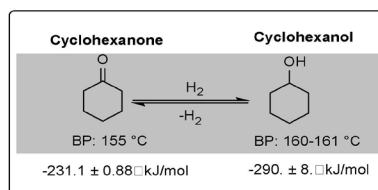


23

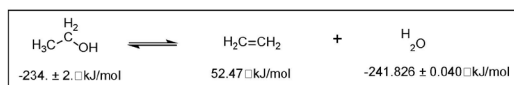
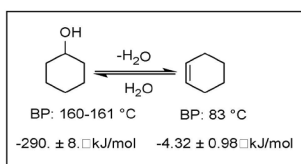


## Reversible Organic Transformations Studied: Alcohols

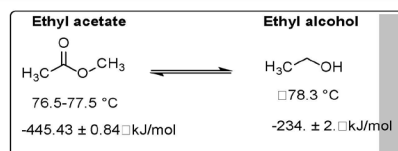
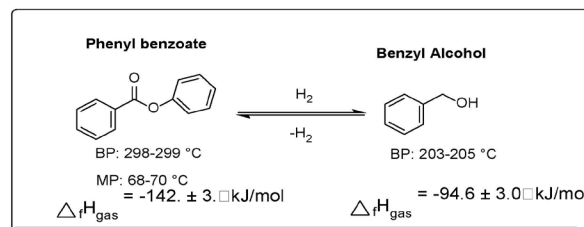
### Dehydrogenation



### Dehydration



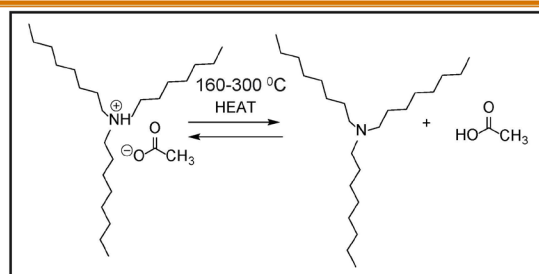
### Esterification



NIST:  $\Delta_f H_{gas}$  Enthalpy of formation of gas at standard conditions



## Reversible Acid-Base Reactions

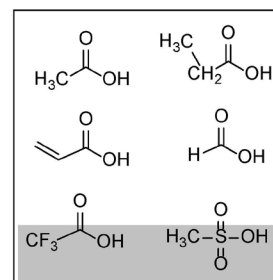


### BASES

Tripropylamine  
Trihexylamine  
Trioctylamine  
Tridodecylamine  
1-Methylimidazole  
Tetramethylguanidine (TMG)

### ACIDS

Acetic Acid  
Propionic acid  
Butanoic acid  
Vinylacetic acid  
Formic acid  
Trifluoroacetic acid  
Methane sulfonic acid



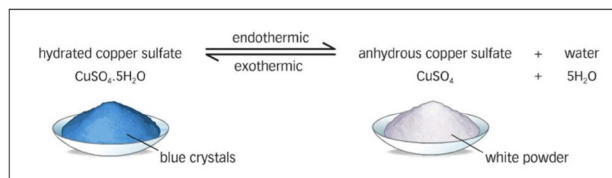
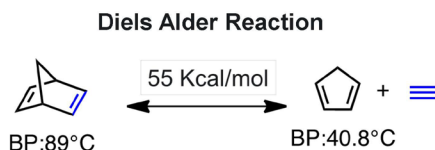
Acids: The alkyl group (CH<sub>3</sub>) in acetic acid can be changed with electron rich and electron poor groups



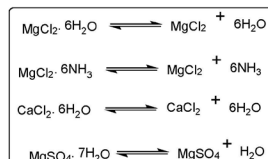
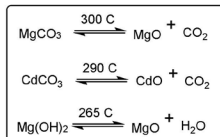


## Reversible Transformations Studied

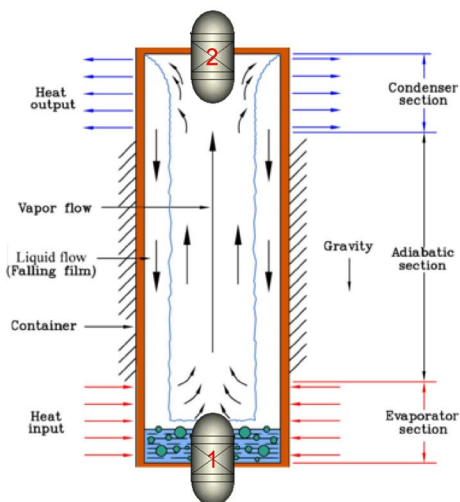
### Inorganic Reactions



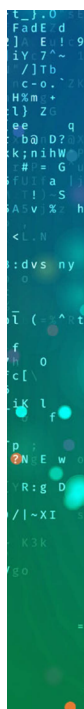
### Silane Hydrolysis



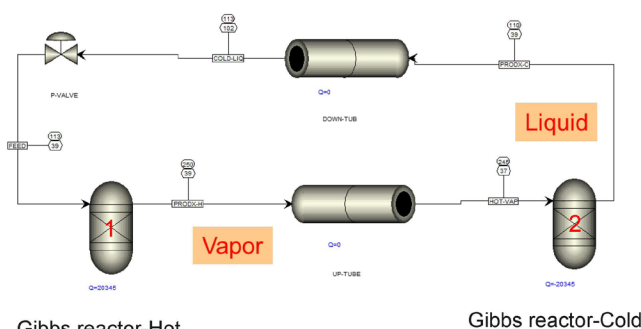
## Heat Pipe Model in Aspen Plus



- Simple steady state model
- Thermodynamic method: Activity coefficient (NRTL etc.) or Equation of State (Peng-Robinson, SRK etc.)
- Use Gibbs reactors to calculate heat duty
- Obtain thermodynamic and thermohydraulic properties
- Identify promising candidates for thermocatalytic heat pipes



## Task 1-Aspen plus model-Ethanol dehydration example

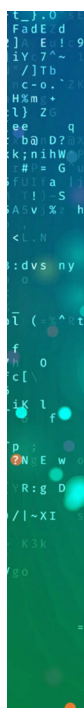


Feed liquid volume: 71.05 L/h  
Enthalpy change: 1198.01 kJ/L

Hot Cold

ETHANOL	0.799	0.049
ETHYLENE	0.101	0.475
WATER	0.101	0.475

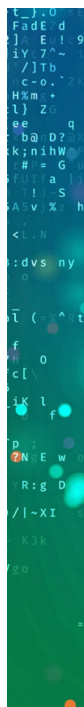
- Use two Gibbs reactors to simulate equilibrium for reactions and neglect kinetics.
- The hot side temperature (250 °C) and cold side temperature (110 °C) is used.
- The initial flowrate of the feed line is set to 1 kmol/hr for the starting and the initial compositions is set to match stoichiometric composition.
- The heat duties of the reactors combining the liquid flow rate are used to estimate the amount of heat that can possibly be extracted per volume base.
- Simulations could not be performed in cases where data on reactants and products was not available



## Task 1-Reaction System Simulations-Results Summary

Reaction	Highest normal b.p. (°C)	Temperature range (°C)	Pressure (atm)	Enthalpy change (kJ/hr)	Feed volume (L/hr)	Enthalpy per volume (MJ/m³)	Effective conversion	*ΔG_foward (kJ/mol)	*ΔG_reverse (kJ/mol)	Both ΔG negative (Y/N)
L-L { Current geothermal power	100	165-75	10	N/A	N/A	360.33	N/A	N/A	N/A	N/A
H <sub>2</sub> O phase change	100	250-110	39	10723	19.90	2254.67	N/A	N/A	N/A	N/A
EtOH phase change	78.4	250-110	39	11611	67.09	724.10	N/A	N/A	N/A	N/A
EtOH dehydration	100	250-110	39	20345	71.05	1198.01	70.5%	-5.49	-11.87	Y
V-L { 1-Propanol dehydration	97	250-110	39	13881	121.98	476.14	2.8%	-20.11	4.51	N
1-Butanol dehydration	117.7	250-110	39	17748	132.94	558.58	0.9%	-22.33	7.25	N
1-Pentanol dehydration	138	250-110	39	21405	134.16	667.55	23.6%	-22.71	8.35	N
Cyclohexanol dehydration	160.9	250-110	39	22063	127.87	721.94	4.8%	-34.29	16.73	N
2,5-Norbornadiene DA	89	250-110	26	12322	108.78	473.93	Negligible	205.40	-219.56	N
S-V { CuSO <sub>4</sub> ·5H <sub>2</sub> O dehydration	650	250-110	39	79425	30.00	11077.14	100%	-16.86	-16.97	Y
V-V { Steam methane reforming (HT)	100	825-600	40	9185	1986.87	19.34	53.8%	-15.47	-37.43	Y
Steam methane reforming (LT)	100	250-110	40	7564	277.69	113.97	0.8%	76.22	-139.07	N

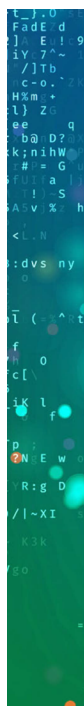
- Ethanol dehydration reaction was most promising in the V-L reaction set
- Low effective conversions under the simulated conditions limited effectiveness of many systems
- Having both forward and reverse reactions with negative ΔG helps achieve a higher conversion efficiency
- Inorganic solid dehydration reaction (CuSO<sub>4</sub>·5H<sub>2</sub>O) looks particularly attractive
  - High reaction enthalpy per unit volume
  - Excellent conversion efficiency
  - High density of reagent
  - Will require dispersal in non-aqueous heat transfer fluid (nanofluid technology)



## Summary

- Several promising thermochemical systems were identified with volumetric reaction enthalpies that are consistent with values that show significant benefit in subsurface reservoir simulations
- From a traditional heat pipe design perspective with V-L reactants/products, ethanol dehydration appears to be a promising candidate
- Exploiting the dehydration of copper sulfate pentahydrate could be very promising provided cycling between the anhydrous and hydrous copper sulfate can be achieved in an appropriate carrier fluid
- Many other potentially promising reaction systems were identified that will require collection of additional thermochemical data to simulate properly with ASPEN Plus and may require development and testing of catalysts that could improve conversion efficiency under relevant geothermal conditions

30



## Overall Conclusions and Recommendations

- Subsurface simulations conclusively illustrate potential of thermochemical heat pipe technology to increase quality of heat brought to the surface from a wide variety of geothermal reservoir types
- Technology offers significant potential to reduce geothermal well field development costs per MW of power generation
- Several thermochemical reaction systems were identified, some of them that avoid need for catalyst development to implement, which could significantly compress R&D timeline from Lab → Field Trial → Commercial Application
- PNNL recommends proceeding with a Phase 2 development effort directed at demonstrating operational performance of selected thermochemical heat pipe systems

31



# **Pacific Northwest National Laboratory**

902 Battelle Boulevard  
P.O. Box 999  
Richland, WA 99354  
1-888-375-PNNL (7665)

***[www.pnnl.gov](http://www.pnnl.gov)***